RSC Advances

PAPER

View Article Online
View Journal | View Issue

Cite this: *RSC Adv.*, 2020, **10**, 746

Cembrane-type diterpenoids from the gum resin of *Boswellia carterii* and their biological activities†

Xiaowei Sun,[ab] Yanling Geng,[a] Xiao Wang,[a] Dawei Qin*[b] and Jinqian Yu*[a]

Eight new cembrane-type diterpenoids, boscartins AH–AK (**1–8**), along with two known ones (**9-10**), were isolated from the gum resin of *Boswellia carterii*. Compounds **1–3** were characteristic of high oxidation assignable to three epoxy groups, while compounds **4–8** were characteristic of two epoxy groups. Spectroscopic examination was used to elucidate their structures. All isolates were evaluated for antiproliferative activity against HCT-116 human colon cancer cells, anti-inflammatory activity against nitric oxide (NO) production, and hepatoprotective activity *in vitro*. All of them showed weak antiproliferative activity (IC_{50} > 100 μM), **8** exhibited potent inhibitory effects on NO production (IC_{50} of 14.8 μM), with the others showing weak anti-inflammatory activity (IC_{50} > 30 μM), and **1** exhibited more potent hepatoprotective activity than the positive control, bicyclol, at 10 μM against the damage induced by paracetamol in HepG2 cells.

Received 22nd November 2019
Accepted 20th December 2019

DOI: 10.1039/c9ra09776g

rsc.li/rsc-advances

1. Introduction

Boswellia carterii Birdw. belonging to the family of Burseraceae is greatly known for its ability to secrete a gum resin by the bark, which was known as olibanum. The gum resin of *Boswellia carterii* has been used in traditional Chinese medicine (TCM) for blood-activating and pain-relieving drugs to treat inflammatory diseases, blood stasis, traumatic injuries, and so on.[1] Previous studies have led to the identification of the active compounds from the gum resin of *Boswellia carterii* mainly as mono-, sesqui-, di- and tri-terpenoids, which have been discovered to show anti-inflammatory, cytotoxic, hepatoprotective, antibacterial, and antifungal activities.[2–10] Among these different kinds of metabolites, diterpenoids and triterpenoids have been identified as the main bioactive ones, which have been mainly classified into the cembrane-type and prenylaromandendrane-type diterpenoids and the oleanane-type and ursane-type triterpenoids. In particular, cembrane-type diterpenoids bearing a 14-membered oxygenated macrocycle have received more and more interest in the laboratory studies of structural modification and natural product research, however, which are mainly contained in soft corals.[11–15] Due to the difficulty of obtaining these soft corals, there has been an increasing research into the cembrane-type diterpenoids obtained from terrestrial plants. Nowadays, more and more pharmacological studies have been carried out to research the chemical diversity of cembrane-type diterpenoids reported from the gum resin of *Boswellia carterii*, the acquisition of which is in great demand from the viewpoints of structural and pharmacological properties.[2,3,16,17]

As part of an ongoing research for cembrane-type diterpenoids with diverse structures and significant activities from the gum resin of *Boswellia carterii*, a phytochemical investigation of the petroleum ether extract was conducted on the basis of the cytotoxic activity against HCT 116 cell, anti-inflammatory activity against nitric oxide (NO) production, and hepatoprotective activity *in vitro*. During this study, eight new cembrane-type diterpenoids (**1–8**) and two known ones (**9-10**)

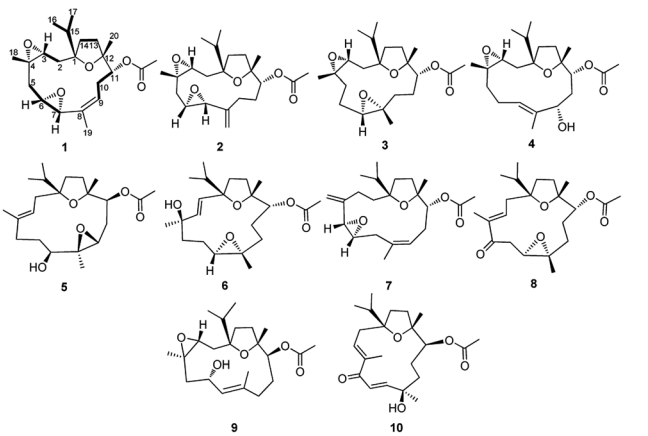

Fig. 1 The structures of **1–10** and key COSY (—) correlations observed for **1**.

[a]*Qilu University of Technology (Shandong Academy of Sciences), Shandong Analysis and Test Center, Shandong Key Laboratory of TCM Quality Control Technology, Jinan, 250014, P. R. China. E-mail: yujinqian87528@126.com*

[b]*School of Chemistry and Pharmaceutical Engineering, Qilu University of Technology (Shandong Academy of Sciences), Jinan 250353, Chin. E-mail: aqdw109@163.com*

† Electronic supplementary information (ESI) available: NMR spectra for theses new compounds. See DOI: 10.1039/c9ra09776g

(Fig. 1) were obtained from the gum resin of *Boswellia carterii*. What's interesting, all the obtained cembrane-type diterpenoids were characteristic of high oxidation assignable to multiple epoxy groups. Herein, the isolation and structural elucidation of the new compounds are discussed, as well as the anti-proliferative activity against HCT-116 human colon cancer cell, anti-inflammatory activity against nitric oxide (NO) production, and protective effect on cytotoxicity induced by paracetamol in HepG2 cells of all the isolated compounds.

2. Results and discussion

The gum resin of *B. carterii* was extracted with 95% ethanol to offer a crude extract, which was further suspended in 20% aqueous ethanol and partitioned successively with petroleum ether (PE), CH_2Cl_2, and EtOAc. The partitioned PE part was eluted rapidly by silica gel chromatography with PE and CH_2Cl_2. The eluted PE part was subjected to multiple column chromatography (CC) to afford eight newly described cembrane-type diterpenes (**1–8**) and two known cembranes (**9-10**). The NMR spectra analysis of these isolated compounds also revealed the characteristic structure category of cembrane-type diterpenoids, with elucidated as preliminary common cembranoid featured by one fourteen-member ring incorporated with one isopropyl.[14,15]

Compound **1** was presented as colorless oil, the molecular formula of which was determined as $C_{22}H_{34}O_5$ based on its positive HRESIMS ion peak at *m*/*z* 379.2505 $[M + H]^+$ (calcd for 379.2440) with six indices of hydrogen deficiency. The IR spectrum suggested the absorption bands for hydroxy (3476 cm^{-1}) and ester carbonyl (1736 cm^{-1}) groups. Its ^1H NMR data (Table 1) displayed signals of one isopropyl at δ_H 0.91 (3H, d, J = 6.8 Hz, Me-16), 0.96 (3H, d, J = 6.8 Hz, Me-17), 2.17 (1H, m, H-15), three methyl singlets at δ_H 1.18 (3H, s, Me-20), 1.34 (3H, s, Me-18) and 1.51 (3H, s, Me-19), one olefinic proton at δ_H 5.43 (1H, dd, J = 6.0, 10.8 Hz, H-9) and four oxymethine protons at δ_H 4.75 (1H, d, J = 10.8 Hz, H-11) and 2.94 (1H, dt, J = 4.0, 8.8 Hz, H-6). Its further analysis of the ^{13}C NMR and HSQC spectra showed signals of five methyls, five methylenes, six methines including one olefinic methine at δ_C 125.3 (C-9), four oxymethines at δ_C 59.2 (C-3), 53.6 (C-6), 56.1 (C-7), 80.9 (C-11), and four quaternary carbons including three oxygenated tertiary carbons at δ_C 89.0 (C-1), 57.7 (C-4), and 83.8 (C-12), and one quaternary olefinic carbon at δ_C 137.9 (C-8). Thus, the aforementioned evidence hinted at the presence of the diagnostic cembrane-type diterpenoid with one isopropyl, three methyl singlets, and one double bond in compound **1**. What's more, one acetyl group was also revealed in compound **1** deduced by δ_H 2.08 (3H, s) and δ_C 170.8, 21.1, in conjuction with IR absorption at 1709 cm^{-1}, assigned to C-11 based on the HMBC correlation of H-11/$CH_3\underline{CO}$.

The cembrane-type planar structure of **1** was unambiguously elucidated by the integrated evidence provided by the 2D NMR experiments. Five different substructural fragments **a** (C-2–C-3), **b** (C-5–C-6–C-7), **c** (C-9–C-10–C-11), **d** (C-13–C-14), **e** (C-15–C-16 and C-15–C-17) were readily identified by the correlations from the COSY spectrum, the connectivities of which were achieved by the HMBC correlations (Fig. 2). Pivotal correlations of H_2-2, H-3, H-15, Me-16 and Me-17 to C-1; H_2-2, H-3, H_2-5, H-6, and Me-18 to C-4; H-6, H-7, H-9, H_2-10, and Me-19 to C-8; H_2-10, H-11, H_2-14, and Me-20 to C-12, H-15 to C-1, C-2, C-12 and C-14 from the HMBC data, confirmed the cyclization of a 14-membered macrocycle but also the linkage of the isopropyl to this macrocycle. Additionally, 3 of 6 degrees of unsaturation were accounted for a double bond, an acetyl carbonyl, and a macrocycle, which allowed the remain three degrees of unsaturation for three additional epoxy rings of 1:12-epoxide, 3:4-epoxide, and 6:7-epoxide, in conjuction with the molecular formula and ^{13}C NMR data. The 8, 9 double bond was located according to the HMBC correlations of H-9/C-7/C-8/C-10/C-11, Me-19/C-7/C-8/C-9, and H-7/C-5/C-8/C-9/Me-19. Thus, the planar structure of **1** was assigned as 1:12,3:4,6:7-triepoxy-11-acetoxy-8-cembranene, which represented the first cembrane-type diterpenoid with three epoxy bridges at 1:12, 3:4, and 6:7.

The configurations and structure of **1** were further established by analysis of its NOESY correlations and coupling constants. The NOE correlations of H-3/H-5b, H-7; H-6/H-7, Me-18, Me-19; H-7/H-3, H-5b; H-10a/Me-20, H-3, H-7, H-11; H-10b/H-9; and H-11/H-3, H-10a, Me-20, showed that H-3, H-6, H-7, H-10a, H-11, Me-18 and Me-20 were all in β, thus, rendering the 3,4-oxirane, 6,7-oxirane and the acetyl group at C-11 to be α orientations (Fig. 3). Additionally, the large coupling constant of $J_{H\text{-}9,H\text{-}10a}$ = 10.8 Hz, and the small coupling constant of $J_{H\text{-}9,H\text{-}10b}$ = 6.0 Hz, as well as the large coupling constant of $J_{H\text{-}11,H\text{-}10b}$ = 10.8 Hz, and the small coupling constant of $J_{H\text{-}11,H\text{-}10a}$ = 0.8 Hz, indicated not only a less than 90° torsional angle between the intersecting H(9)C(9)C(8) and H(10b)C(10)C(9) flats, but also a approximately 180° torsional angle between the intersecting H(10b)C(10)C(11) and H(11)C(11)C(10) flats (Fig. 3), ascertaining the α orientation of the acetyl group at C-11. Similarly, the large coupling constant of $J_{H\text{-}5b,H\text{-}6}$ = 10.4 Hz, and the small coupling constant of $J_{H\text{-}5a,H\text{-}6}$ = 4.0 Hz, as well as the large coupling constant of $J_{H\text{-}5a,H\text{-}5b}$ = 13.2 Hz, and the singlet of H-7, indicated not only a approximately 180° torsional angle between the intersecting H(6)C(6)C(5) and H(5b)C(5)C(6) flats, but also the α orientation of the 6,7-oxirane group (Fig. 3). In addition, the olefinic geometry of C-8/C-9 was ascertained as *Z* form by the NOE correlations of H-9/Me-19. Hence, the structure of **1** was defined as (1*S*,3*R*,4*S*,6*R*,7*R*,11*R*,12*R*,8*Z*)-1:12,3:4,6:7-triepoxy-11-acetoxy-8-cembrene (boscartins AH) with the aid of a computer-modeled 3D structure (Fig. 3) generated by MM2 force field calculations for energy minimization using the molecular modeling program Chem 3D Ultra 14.0.

Compound **2** was presented as colorless oil with the molecular formula of $C_{22}H_{34}O_5$ as determined to be the same with **1** by its positive HRESIMS experiment (*m*/*z* 379.2521 $[M + H]^+$, calcd for 379.2440), with six indices of hydrogen deficiency. The IR spectrum suggested the absorption bands for hydroxy (3395 cm^{-1}) and ester carbonyl (1733 cm^{-1}) groups. The ^1H and ^{13}C NMR data of **2** were detailedly compared with those of **1**, evidencing that **2** was an isomer of **1**, which was further confirmed by the integrated evidence provided by the 1D and 2D NMR experiments (Table 1). The ^1H NMR data of **2** established

Table 1 ^{1}H (400 MHz) and ^{13}C (100 MHz) NMR data for compounds **1–4** (δ in ppm, J in Hz)[a]

	1		**2**		**3**		**4**	
No.	δ_H[a]	δ_C[a]	δ_H	δ_C	δ_H	δ_C	δ_H	δ_C
1		89.0		88.2		88.9		88.9
2a	2.01 m	36.4	1.84 d(15.2)	35.1	1.95 d(15.2)	36.4	1.83 dd(3.2, 15.2)	35.3
2b	1.64 overlapped		1.60 dd(10.4, 15.2)		1.60 overlapped		1.58 dd(5.2, 15.2)	
3	3.06 dd(2.4, 4.0)	59.2	3.08 d(10.4)	57.8	3.14 t(3.2)	60.1	2.92 dd(3.2, 5.2)	59.4
4		57.7		57.2		58.8		59.2
5a	2.79 dd(4.0, 13.2)	42.9	2.61 dd(2.4, 13.8)	41.4	1.65 overlapped	36.0	2.11 m	37.2
5b	0.78 dd(13.2, 10.4)		1.08 dd(10.4, 13.8)		1.42 m		1.45 overlapped	
6a	2.94 dt(8.8, 4.0)	53.6	2.73 d(10.4)	60.1	1.81 m	25.2	2.25 m(2H)	23.4
6b					1.67 m			
7	3.56 s	56.1	3.03 s	57.8	3.03 dd(3.6, 6.4)	58.8	5.59 t(6.8)	128.8
8		137.9		143.2		59.9		134.5
9a	5.43 dd(6.0, 10.8)	125.3	2.38 m	32.3	1.61 overlapped	30.6	4.10 d(10.8)	87.2
9b			2.20 m		1.58 overlapped			
10a	2.86 td(0.8, 10.8)	27.6	2.15 m	26.5	1.72 m	23.8	2.07 d(12.8)	31.9
10b	2.14 td(10.8, 6.0)		1.90 m		1.49 m		1.82 dt(12.8, 10.8)	
11	4.75 d(10.8)	80.9	4.82 dd(1.6, 11.6)	76.3	4.84 d(11.2)	79.4	4.78 d(10.8)	76.1
12		83.8		84.1		84.1		83.0
13a	1.96 overlapped	35.7	1.97 overlapped	31.5	1.93 overlapped	35.6	1.88 overlapped	35.4
13b	1.64 overlapped		1.58 overlapped		1.65 overlapped		1.65 overlapped	
14a	1.95 overlapped	30.0	1.97 overlapped	35.4	1.94 overlapped	29.9	1.89 overlapped	29.8
14b	1.64 overlapped		1.66 m		1.43 m		1.46 overlapped	
15	2.17 m	32.7	1.99 overlapped	34.5	1.80 overlapped	32.9	2.09 overlapped	33.0
16	0.91 d(6.8)	18.7	0.91 d(6.8)	17.9	0.93 d(6.8)	18.8	0.90 overlapped	17.1
17	0.96 d(6.8)	16.8	0.94 d(6.8)	17.6	0.95 d(6.8)	16.9	0.90 overlapped	17.1
18	1.34 s	17.9	1.34 s	18.3	1.27 s	19.2	1.23 s	17.1
19	1.51 s	17.6	4.92 s, 4.74 s	110.8	1.27 s	17.0	1.73 s	14.5
20	1.18 s	21.5	1.20 s	22.4	1.10 s	21.5	1.16 s	21.5
$\underline{CH_3}CO$	2.08 s	21.1	2.10 s	21.1	2.09 s	21.2	2.11 s	21.3
$CH_3\underline{CO}$		170.8		170.6		171.2		171.3
OH							7.93 s (OH-9)	

[a] ^{1}H and ^{13}C NMR spectra were obtained in $CDCl_3$.

not only the replacement of an olefinic methine in **1** by an exo methylene at δ_H 2.38 and 2.20 (H_2-9), but also the replacement of an allylic methyl in **1** by a olefinic exomethylene at δ_H 4.92 and 4.74 (H_2-19). The ^{13}C NMR data of **2** established the replacement of trisubstituted double bond at C_8–C_9 in **1** by a *gem*-disubstituted double bond at C_8–C_{19} [C-8 (δ_C 143.2) and C-19 (δ_C 110.8)]. Additionally, the HMBC correlations of H_2-9 to C-7 (δ_C 57.8), C-8, C-10 (δ_C 26.5), C-11 (δ_C 76.3), C-19, and H_2-19 to C-7, C-8, C-9, confirmed the location of the double bond at C_8–C_{19}. Thus, the planar structure of **2** was assigned as 1:12,3:4,6:7-triepoxy-11-acetoxy-8,19-cembranene.

The configurations and structure of **2** were further established by analysis of its NOESY correlations and coupling constants. The NOE correlations of H-3/H-2a, H-5b, H-6, H-11, Me-16; H-2a/Me-18; H-5b/H-3, H-7, Me-16, Me-17; H-6/H-9b, H-11, H-19, Me-18; H-7/H-5b, H-11; and H-11/H-3, H-6, Me-18, Me-20, showed that H-3, H-2a, H-5b, H-6, H-7, H-11, Me-18 and Me-20 were all in β, thus, rendering the 3,4-oxirane, 6,7-oxirane and the acetyl group at C-11 to be α orientations (Fig. 3). Additionally, the large coupling constant of $J_{H\text{-}3,H\text{-}2b} = 10.4$ Hz, $J_{H\text{-}5a,H\text{-}5b} = 13.8$ Hz, $J_{H\text{-}6,H\text{-}5b} = 10.4$ Hz, $J_{H\text{-}11,H\text{-}10b} = 11.6$ Hz, and the small coupling constant of $J_{H\text{-}5a,H\text{-}6} = 2.4$ Hz, $J_{H\text{-}6,H\text{-}7} = 0$ Hz, $J_{H\text{-}11,H\text{-}10a} = 1.6$ Hz, as well as the biogenetic consideration, also indicated the above assigned orientations for H-3, H-6, H-7, H-11. Hence, the structure of **2** was defined as (1*S*,3*R*,4*S*,6*R*,7*R*,11*R*,12*R*)-1:12,3:4,6:7-triepoxy-11-acetoxy-8,19-cembrene (boscartins AI) with the aid of a computer-modeled 3D structure (Fig. 3) generated by MM2 force field calculations for energy minimization using the molecular modeling program Chem 3D Ultra 14.0.

Compound **3** was presented as colorless oil with the molecular formula of $C_{22}H_{36}O_5$ as determined by its positive HRESIMS experiment (m/z 381.2653 $[M + H]^+$, calcd for 381.2596), with five indices of hydrogen deficiency. The IR spectrum suggested the absorption bands for hydroxy (3455 cm^{-1}) and ester carbonyl (1734 cm^{-1}) groups. The ^{1}H and ^{13}C NMR data of **3** were carefully compared with those of **1**, clearly evidencing the consistent 1:12,3:4-diepoxy-11-acetoxy-containing cembrane type backbone between them, with the difference ascribed to signals at C-6 (δ_C 25.2), C-7 (δ_C 58.8), C-8 (δ_C 59.9), and C-9 (δ_C 30.6). The ^{1}H NMR data of **3** established not only the replacement of an oxymethine in **1** by an exo methylene at δ_H 1.81 and 1.67 (H_2-6), but also the replacement of an olefinic methine in **1** by an exo methylene at δ_H 1.61 and 1.58 (H_2-9). The ^{13}C NMR

data of **3** established the epoxy ring of 6:7-epoxide in **1** was migrated to C-7 and C-8 in **3**, and the trisubstituted double bond at C_8–C_9 in **1** was hydrogenised in **3**. In-depth 2D NMR scrutiny established the above deduction. Obviously, the notable HMBC correlations of H-7 (δ_H 3.03) to C-5 (δ_C 36.0), C-6, C-8, C-9, Me-19 (δ_C 17.0) and Me-19 (δ_H 1.27) to C-7, C-8, C-9 indicated an oxygen bridge between C-7 and C-8, constructing a 1:12,3:4,7:8-triepoxy-11-acetoxy-cembrane motif for **3**.

The configurations and structure of **3** were further established by analysis of its NOESY correlations and coupling constants. The NOE correlations of H-3/H-15, Me-16, Me-17; H-7/H-11, Me-16, Me-17, Me-18, Me-19; H-11/H-7, H-10a, Me-18, Me-19, Me-20, showed that H-3, H-7, H-11, Me-18, Me-19 and Me-20 were all in β, thus, rendering the 3,4-oxirane, 7,8-oxirane and the acetyl group at C-11 to be α orientations (Fig. 3). Additionally, the large coupling constant of $J_{H\text{-}11,H\text{-}10b} = 11.2$ Hz also indicated the above assigned orientation for H-11. Hence, the structure of **3** was defined as (1*S*,3*R*,4*S*,7*R*,8*S*,11*R*,12*R*)-1:12,3:4,7:8-triepoxy-11-acetoxy-cembrane (boscartins AJ) with the aid of a computer-modeled 3D structure (Fig. 3) generated by MM2 force field calculations for energy minimization using the molecular modeling program Chem 3D Ultra 14.0, as well as the biogenetic consideration.

Compound **4** was presented as colorless oil with the molecular formula of $C_{22}H_{36}O_5$ as determined by its positive HRESIMS experiment (*m*/*z* 379.2357 $[M - H]^-$, calcd for 381.2596), with five indices of hydrogen deficiency. The IR spectrum suggested the absorption bands for hydroxy (3454 cm^{-1}) and ester carbonyl (1737 cm^{-1}) groups. The ^1H and ^{13}C NMR data of **4** were carefully compared with those of **9** (boscartins Q), clearly evidencing the resembled 1:12,3:4-diepoxy-11-acetoxy-7-cembranene type backbone between them. The only difference between them was ascribed to the migration of a hydroxy group from C-6 in **9** to C-9 in **4**, which was further supported by the well-resolved HMBC correlations of H-6 (δ_H 2.25)/C-4 (δ_C 59.2), C-5 (δ_C 37.2), C-7 (δ_C 128.8), C-8 (δ_C 134.5); H-7 (δ_H 5.59)/C-5, C-6 (δ_C 23.4), C-9 (δ_C 87.2), Me-19 (δ_C 14.5); H-9 (δ_H 4.10)/C-7, C-8, C-10 (δ_C 31.9), C-11 (δ_C 76.1), Me-19; H-11 (δ_H 4.78)/C-9, C-10, C-12 (δ_C 83.0), C-13 (δ_C 35.4), Me-20 (δ_C 21.5), $\underline{CO}CH_3$ (δ_C 171.3); Me-19 (δ_H 1.73)/C-7, C-8, C-9, thus, constructing a 1:12,3:4-diepoxy-11-acetoxy-7-cembranene-9-ol motif for **4**.

The configurations and structure of **4** were further established by analysis of its NOESY correlations and coupling constants, as well as comparison those with **9**. The NOE correlations of H-3/H-7, H-11, H-15, Me-16, Me-17, Me-18; H-9/H-7, H-10a, H-11; H-11/H-3, H-9, H-10a, Me-20; Me-18/H-3 showed that H-3, H-9, H-11, Me-18 and Me-20 were all in β, thus, rendering the 3,4-oxirane, the hydroxy group at C-9 and the acetyl group at C-11 to be α orientations (Fig. 3). The NOE correlations of H-11 and Me-18 were opposite to those observed in **9**, further ascertaining the above orientations for H-3, H-9, H-11, and Me-18. Additionally, the large coupling constants of $J_{H\text{-}9,H\text{-}10b} = 10.8$ Hz, $J_{H\text{-}11,H\text{-}10b} = 10.8$ Hz, and $J_{H\text{-}10a,H\text{-}10b} = 12.8$ Hz, as well as the little coupling of H-9/H-10a and H-11/H-10a, indicated an approximately 180° torsional angle not only between the intersecting H(9)C(9)C(10) and H(10b)C(10)C(9) flats, but also between the intersecting H(10b)C(10)C(11) and H(11)C(11)C(10) flats (Fig. 3), ascertaining the α orientations for the hydroxy group at C-9 and the acetyl group at C-11. Based on the NOE correlations of H-7/H-3 and Me-19/H-9, the olefinic geometry of C-7/C-8 was ascertained as *E* form. Hence, the structure of **4** was defined as (1*S*,3*R*,4*S*,9*S*,11*R*,12*R*,8*E*)-1:12,3:4-diepoxy-11-acetoxy-7-cembranene-9-ol (boscartins AK) with the aid of a computer-modeled 3D structure (Fig. 3) generated by MM2 force field calculations for energy minimization using the molecular modeling program Chem 3D Ultra 14.0, as well as the biogenetic consideration.

Compound **5** was presented as colorless oil with the molecular formula of $C_{22}H_{36}O_5$ as determined to be the same with **4** by its positive HRESIMS experiment (*m*/*z* 381.2635 $[M + H]^+$, calcd for 381.2596), with five indices of hydrogen deficiency. The IR spectrum suggested the absorption bands for hydroxy (3425 cm^{-1}) and ester carbonyl (1731 cm^{-1}) groups. The ^1H and ^{13}C NMR data of **5** were detailedly compared with those of **4**, evidencing that **5** was an isomer of **4**, which was further

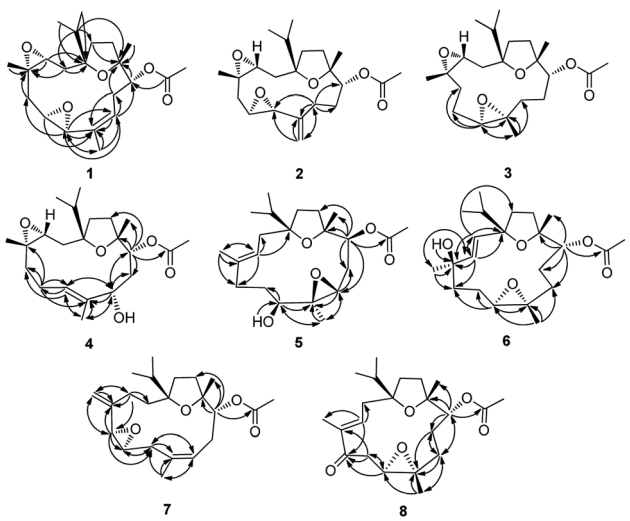

Fig. 2 Key HMBC (⟶) correlations observed for **1**–**8**.

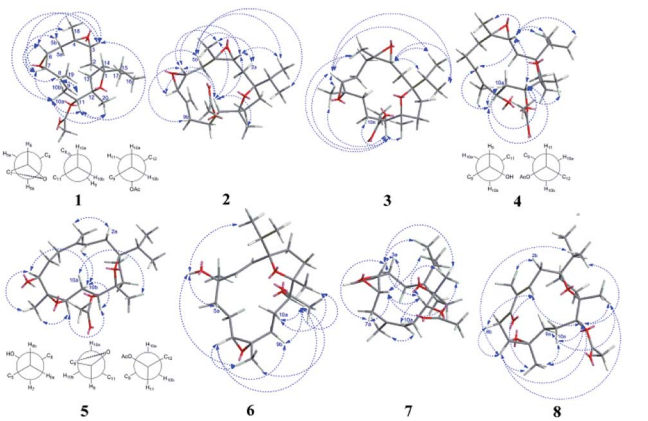

Fig. 3 Key NOE (⇠⇢) correlations observed for **1**–**8** (3D structures of **1**–**8** were generated by MM2 force field calculations for energy minimization using the molecular modeling program Chem 3D Ultra 14.0).

confirmed by the integrated evidence provided by the 1D and 2D NMR experiments (Table 1). The ^{1}H NMR data of **5** established not only the replacement of an oxymethine in **4** by an olefinic methine at δ_H 5.12 (H-3), but also the replacement of an olefinic methine in **4** by an oxymethine at δ_H 3.66 (H-7). The ^{13}C NMR data of **5** established the replacement of an epoxy ring of 3:4-epoxide in **4** by a trisubstituted double bond at C_3–C_4 in **5** [C-3 (δ_C 118.9) and C-4 (δ_C 135.4)], the replacement of a trisubstituted double bond at C_7–C_8 in **4** by an oxymethine at C-7 (δ_C 69.7) and a nonprotonated oxygenated tertiary carbon at C-8 (δ_C 64.8). Additionally, the HMBC correlations of H-3 to C-1 (δ_C 89.2), C-2 (δ_C 28.8), C-5 (δ_C 32.3), Me-18 (δ_C 18.7); H-7 to C-6 (δ_C 31.2), C-8, Me-19 (δ_C 16.4); OH-7 (δ_H 4.25) to C-7; H-9 (δ_H 2.71) to C-8, C-10 (δ_C 27.7), Me-19; H-11 to C-9 (δ_C 63.8), C-10, C-12 (δ_C 82.8), C-13 (δ_C 35.3), Me-20 (δ_C 22.3), $\underline{CO}CH_3$ (δ_C 170.9); Me-18 (δ_H 1.64) to C-3, C-4, C-5; Me-19 (δ_H 1.27) to C-7, C-8, C-9, confirmed the location of the double bond at C_3–C_4, the hydroxy group at C-7, and the epoxy ring at C_8–C_9, in association with the five degrees of unsaturation. Thus, the planar structure of **5** was assigned as 1:12,8:9-diepoxy-11-acetoxy-3-cembranene-6-ol.

The configurations and structure of **5** were further established by analysis of its NOESY correlations and coupling constants, as well as comparison those with **4**. The NOE correlations of H-7/H-10b, Me-19; H-9/H-11, Me-19; H-11/H-9, H-10b; H-10a/Me-20, in association with the absence of H-11/Me-20, and H-7/Me-20, showed that H-10a and Me-20 were both in β, and H-7, H-9, H-11, and Me-19 were all in α, thus, rendering the hydroxy group at C-7, the 8,9-oxirane, and the acetyl group at C-11 to be β orientations (Fig. 3). The NOE correlations of H-11 were opposite to those observed in **4**, further ascertaining the above orientations for H-7, H-9, H-11, and Me-19. Additionally, the large coupling constants of $J_{H\text{-}7,H\text{-}6b}$ = 10.0 Hz, $J_{H\text{-}9,H\text{-}10a}$ = 10.8 Hz, and $J_{H\text{-}11,H\text{-}10a}$ = 11.6 Hz, as well as small coupling constant of $J_{H\text{-}9,H\text{-}10b}$ = 3.2 Hz and the little coupling of H-7/H-6a and H-11/H-10b, indicated an approximately 180° torsional angle between the intersecting H(6b)C(6)C(7) and H(7)C(7)C(6) flats, between the intersecting H(9)C(9)C(10) and H(10a)C(10)C(9) flats, between the intersecting H(10a)C(10)C(11) and H(11)C(11)C(10) flats (Fig. 3), ascertaining the β orientations for the hydroxy group at C-9, the epoxy ring at C_8–C_9, and the acetyl group at C-11. Based on the NOE correlations of H-3/H-10b and Me-18/H-2a, the olefinic geometry of C-3/C-4 was ascertained as *E* form. Hence, the structure of **5** was defined as (1*S*,7*S*,8*S*,9*R*,11*S*,12*R*,3*E*)-1:12,8:9-diepoxy-11-acetoxy-3-cembranene-7-ol (boscartins AL) with the aid of a computer-modeled 3D structure (Fig. 3) generated by MM2 force field calculations for energy minimization using the molecular modeling program Chem 3D Ultra 14.0, as well as the biogenetic consideration.

Compound **6** was presented as colorless oil with the molecular formula of $C_{22}H_{36}O_5$ as determined to be the same with **4** and **5** by its positive HRESIMS experiment (*m*/*z* 403.2455 [M + Na]$^+$, calcd for 403.2460), with five indices of hydrogen deficiency. The IR spectrum suggested the absorption bands for hydroxy (3427 cm^{-1}) and ester carbonyl (1733 cm^{-1}) groups. The ^{1}H and ^{13}C NMR data of **6** were detailedly compared with those of **4** and **5**, evidencing that **6** was an isomer of **4** and **5**, which was further confirmed by the integrated evidence provided by the 1D and 2D NMR experiments (Table 2). The ^{1}H NMR data of **6** established not only the replacement of an exo methylene in **5** by an olefinic methine at δ_H 5.69 (H-2), but also the replacement of an oxymethine in **5** by an exo methylene at δ_H 1.99, 0.89 (H_2-9). The ^{13}C NMR data of **6** established the migration of a double bond from C_3–C_4 in **5** to C_2–C_3 [C-2 (δ_C 135.9), C-3 (δ_C 131.2)], and the replacement of a trisubstituted olefinic carbon at C_4 in **5** by a nonprotonated oxygenated tertiary carbon at C-4 (δ_C 81.3), as well as the migration of an epoxy ring from C_8–C_9 in **5** to C_7–C_8 [C-7 (δ_C 64.4), C-8 (δ_C 61.4) and C-9 (δ_C 34.3)]. Additionally, the HMBC correlations of H-2 to C-1 (δ_C 88.9), C-3, C-4, C-14 (δ_C 34.4); H-3 (δ_H 5.63) to C-1, C-2, C-4, C-5 (δ_C 35.0), Me-18 (δ_C 23.4); OH-4 (δ_H 10.83) to C-4; H-7 (δ_H 2.91) to C-5, C-6 (δ_C 21.9), C-8; H-11 (δ_H 4.91) to C-9 (δ_C 34.3), C-10 (δ_C 25.8), C-12 (δ_C 83.6), Me-20 (δ_C 21.2), $\underline{CO}CH_3$ (δ_C 171.2); Me-18 (δ_H 1.30) to C-3, C-4, C-5; Me-19 (δ_H 1.30) to C-7, C-8, C-9, confirmed the location of the double bond at C_2–C_3, the hydroxy group at C-4, and the epoxy ring at C_7–C_8, in association with the five degrees of unsaturation. Thus, the planar structure of **6** was assigned as 1:12,7:8-diepoxy-11-acetoxy-2-cembranene-4-ol.

The configurations and structure of **6** were further established by analysis of its NOESY correlations and coupling constants, as well as comparison those with **4** and **5**. The NOE correlations of OH-4/H-5a, Me-16, Me-19; H-7/H-9b, H-11, Me-19; H-11/H-7, H-9b, H-10a, Me-19, Me-20; H-10a/Me-20, showed that OH-4, H-7, H-11, Me-19 and Me-20 were both in β, and Me-18 was in α, thus, rendering the hydroxy group at C-4, the 7,8-oxirane, and the acetyl group at C-11 to be α orientations (Fig. 3). Additionally, the large coupling constant of $J_{H\text{-}11,H\text{-}10b}$ = 9.6 Hz, as well as the little coupling of H-11/H-10b, ascertained the β orientation for the hydroxy group at C-4, as well as the α orientations for the epoxy ring at C_7–C_8 and the acetyl group at C-11. Based on the large coupling constant of $J_{H\text{-}2,H\text{-}3}$ = 15.6 Hz, the olefinic geometry of C-2/C-3 was ascertained as *E* form. Hence, the structure of **6** was defined as (1*S*,4*R*,7*S*,8*R*,11*R*,12*R*,2*E*)-1:12,7:8-diepoxy-11-acetoxy-2-cembranene-4-ol (boscartins AM) with the aid of a computer-modeled 3D structure (Fig. 3) generated by MM2 force field calculations for energy minimization using the molecular modeling program Chem 3D Ultra 14.0, as well as the biogenetic consideration.

Compound **7** was presented as colorless oil with the molecular formula of $C_{22}H_{34}O_4$ as determined by its positive HRESIMS experiment (*m*/*z* 385.2346 [M + Na]$^+$, calcd for 385.2355), with six indices of hydrogen deficiency. The IR spectrum suggested the absorption bands for hydroxy (3442 cm^{-1}) and ester carbonyl (1731 cm^{-1}) groups. The ^{1}H and ^{13}C NMR data of **7** were detailedly compared with those of **1**, clearly evidencing the consistent 1:12-triepoxy-11-acetoxy-8-cembranene type backbone between them, with the difference ascribed to signals at C-3 (δ_C 30.8), C-4 (δ_C 146.4), C-5 (δ_C 58.5), C-7 (δ_C 40.9) and Me-18 (δ_C 109.4). The ^{1}H NMR data of **7** established the replacement of an oxymethine in **1** by an exo methylene at δ_H 2.37 and 1.99 (H_2-3), the replacement of an exo methylene in **1** by an oxymethine at δ_H 3.18 (H-5), the replacement of an oxymethine in **1** by an exo methylene at δ_H 2.75 and 1.86 (H_2-7), and the replacement of a methyl in **1** by an olefinic exomethylene at δ_H 4.92 and 4.81

(H_2-18). The ^{13}C NMR data of **7** established the epoxy ring of 3:4-epoxide and the linked methyl at C-18 in **1** were transformed into an exo methylene at C-3 and a *gem*-disubstituted double bond at C_4–C_{18}, and the migration of an epoxy ring from C_6–C_7 in **1** to C_5–C_6 [C-5, C-6 (δ_C 62.4), C-7]. In-depth 2D NMR scrutiny established the above deduction. Obviously, the notable HMBC correlations of H-3 to C-2 (δ_C 28.5), C-4, C-5, Me-18; H-5 to C-4, C-6, C-7, Me-18; H-6 (δ_H 2.90) to C-7; H-7a (δ_H 2.75) to C-6, C-8 (δ_C 133.7), C-9 (δ_C 120.6); H-9 (δ_H 5.31) to C-7, Me-19 (δ_C 17.9); H-11 (δ_H 4.93) to C-12 (δ_C 83.5), C-13 (δ_C 35.8), Me-20 (δ_C 22.9), $CH_3\underline{CO}$ (δ_C 171.3); H_2-18 to C-3, C-4, C-5; Me-19 (δ_H 1.64) to C-7, C-8, C-9, indicated a *gem*-disubstituted double bond at C_4–C_{18}, an oxygen bridge between C-5 and C-6, and a trisubstituted double bond at C_8–C_9, constructing a 1:12,5:6-diepoxy-11-acetoxy-4(18),7-cembrandien motif for **7**.

The configurations and structure of **7** were further established by analysis of its NOESY correlations and coupling constants, as well as comparison those with **1**. The NOE correlations of H-5/H-3a, H-7a, H-11, Me-16, Me-20; H-6/H-3a, H-7a, H-11, Me-17, Me-20; H-11/H-5, H-10a, Me-20, showed that H-5, H-6, H-11, Me-16, Me-17 and Me-20 were both in β, thus, rendering the 5,6-oxirane, and the acetyl group at C-11 to be α orientations (Fig. 3). Additionally, the large coupling constant of $J_{H\text{-}6,H\text{-}7b} = 9.6$ Hz, $J_{H\text{-}7a,H\text{-}7b} = 16.8$ Hz, $J_{H\text{-}9,H\text{-}10b} = 9.6$ Hz, $J_{H\text{-}11,H\text{-}10b} = 9.6$ Hz, as well as the little coupling of H-5/H-6 and the small coupling constant of $J_{H\text{-}6,H\text{-}7a} = 2.0$ Hz, $J_{H\text{-}9,H\text{-}10a} = 5.6$ Hz, $J_{H\text{-}11,H\text{-}10a} = 3.2$ Hz, ascertained the α orientations for the epoxy ring at C_5–C_6 and the acetyl group at C-11. Based on the NOE correlations of H-9/Me-19, the olefinic geometry of C-8/C-9 was ascertained as *Z* form. Hence, the structure of **7** was defined as (1*R*,5*R*,6*R*,11*R*,12*R*,8*Z*)-1:12,5:6-diepoxy-11-acetoxy-4(18),7-cembrandien (boscartins AN) with the aid of a computer-modeled 3D structure (Fig. 3) generated by MM2 force field calculations for energy minimization using the molecular modeling program Chem 3D Ultra 14.0, as well as the biogenetic consideration.

Compound **8** was presented as colorless oil with the molecular formula of $C_{22}H_{34}O_5$ as determined by its positive HRESIMS experiment (*m*/*z* 379.2487 $[M + H]^+$, calcd for 379.2440), with six indices of hydrogen deficiency. The IR spectrum suggested the absorption bands for hydroxy (3448 cm^{-1}), ester carbonyl (1737 cm^{-1}), and conjugated carbonyl (1687 cm^{-1})

Table 2 ^1H (400 MHz) and ^{13}C (100 MHz) NMR data for compounds **5**–**8** (δ in ppm, *J* in Hz)

	5[a]		**6**[b]		**7**[a]		**8**[a]	
No.	δ_H	δ_C	δ_H	δ_C	δ_H	δ_C	δ_H	δ_C
1		89.2		88.9		89.9		89.8
2a	2.32 dd(5.6, 16.0)	28.8	5.69 d(15.6)	135.9	1.89 m	28.5	2.47 dd(6.0, 14.0)	31.5
2b	1.97 dd(5.6, 16.0)				1.87 m		2.38 dd(10.0, 14.0)	
3a	5.12 t(5.6)	118.9	5.63 d(15.6)	131.2	2.37 m	30.8	6.54 dd(6.0, 9.2)	141.1
3b					1.99 m			
4		135.4		81.3		146.4		141.1
5a	2.23 m	32.3	2.13 m	35.0	3.18 s	58.5		198.8
5b	2.17 m		1.74 overlapped					
6a	1.85 overlapped	31.2	1.74 overlapped	21.9	2.90 dt(9.6, 2.0)	62.4	2.95 dd(8.8, 13.6)	40.6
6b	1.76 overlapped		1.55 overlapped				2.82 d(13.6)	
7a	3.66 d(10.0)	69.7	2.91 t(5.6)	64.4	2.75 d(16.8)	40.9	3.25 d(8.4)	59.8
7b					1.86 overlapped			
8		64.8		61.4		133.7		61.7
9a	2.71 dd(3.2, 10.8)	63.8	1.99 overlapped	34.3	5.31 dd(5.6, 9.6)	120.6	2.06 m	34.1
9b			0.89 m				0.96 m	
10a	2.11 dt(11.6, 2.8)	27.7	1.90 overlapped	25.8	2.21 dd(5.6, 14.4)	29.3	1.93 m	25.1
10b	2.14 t(11.6)		1.53 overlapped		2.11 dt(9.6, 14.4)		1.63 overlapped	
11	4.90 d(11.6)	74.4	4.91 d(9.6)	77.1	4.93 dd(3.2, 9.6)	76.4	4.70 d(10.8)	74.2
12		82.8		83.6		83.5		83.2
13a	1.76 overlapped	35.3	1.55 overlapped (2H)	35.6	1.74 overlapped	35.8	1.67 overlapped (2H)	34.9
13b	1.71 overlapped				1.70 overlapped			
14a	1.80 overlapped	31.0	1.84 overlapped (2H)	34.4	1.73 overlapped(2H)	30.3	1.78 overlapped	30.7
14b	1.76 overlapped						1.66 overlapped	
15	1.76 overlapped	36.0	1.65 m	38.2	1.80 m	36.3	1.83 m	36.8
16	0.87 d(6.8)	19.0	0.81 t(6.8) (6H)	18.8	0.88 d(6.8)	19.0	0.93 d(6.8)	19.0
17	0.95 d(6.8)	16.7	0.81 t(6.8) (6H)	17.7	0.97 d(6.8)	16.7	1.01 d(6.8)	16.8
18	1.64 s	18.7	1.30 s(6H)	23.4	4.92 s, 4.81 s	109.4	1.79 s	11.8
19	1.27 s	16.4	1.30 s(6H)	16.9	1.64 s	17.9	1.44 s	17.0
20	1.23 s	22.3	1.05 s	21.2	1.20 s	22.9	1.18 s	22.0
$\underline{CH_3}CO$	2.10 s	21.1	2.00 s	21.3	2.10 s	21.2	2.00 s	21.0
$CH_3\underline{CO}$		170.9		171.2		171.3		171.0
OH	4.79 d(4.8) (OH-7)		10.78 s(OH-4)					

[a] ^1H and ^{13}C NMR spectra were obtained in $CDCl_3$. [b] ^1H and ^{13}C NMR spectra were obtained in DMSO-d_6.

groups. The ^{1}H and ^{13}C NMR data of **8** were detailedly compared with those of **10** (boscartins Z), clearly evidencing the consistent 1:12-triepoxy-11-acetoxy-5-oxo-3-cembranene type backbone between them, with the difference ascribed to signals at C-6 (δ_C 40.6), C-7 (δ_C 59.8), and C-8 (δ_C 61.7). The ^{1}H NMR data of **8** established the replacement of an olefinic methine in **10** by an exo methylene at δ_H 2.95 and 2.82 (H_2-6), and the replacement of an olefinic methine in **10** by an oxymethine at δ_H 3.25 (H-7). The ^{13}C NMR data of **8** established the replacement of a double bond in **10** by an exo methylene and an oxymethine at C-6 and C-7. In-depth 2D NMR scrutiny established the above deduction. Obviously, the notable HMBC correlations of H-3 (δ_H 6.54) to C-2 (δ_C 31.5), C-5 (δ_C 198.8), Me-18 (δ_C 11.8); H-6 to C-4 (δ_C 141.1), C-5, C-7; H-7 to C-5, C-6; H-9a (δ_H 2.06) to C-8, C-10 (δ_C 25.1), C-11 (δ_C 74.2), Me-19 (δ_C 17.0); H-10a (δ_H 1.93) to C-8, C-9 (δ_C 34.1); H-11 (δ_H 4.70) to C-9, C-10, C-12 (δ_C 83.2), Me-20 (δ_C 22.0), $CH_3\underline{CO}$ (δ_C 171.0); Me-19 (δ_H 1.44) to C-7, C-8, C-9, indicated a trisubstituted double bond at C_3–C4, a keto at C-5, an oxygen bridge between C-7 and C-8, in association with the six degrees of unsaturation. Thus, the planar structure of **8** was assigned as 1:12,7:8-diepoxy-11-acetoxy-5-oxo-3-cembranene.

The configurations and structure of **8** were further established by analysis of its NOESY correlations and coupling constants, as well as comparison those with **10**. The NOE correlations of H-7/H-6b, H-11, Me-17, Me-19, Me-20; H-11/H-3, H-7, H-10a, Me-17, Me-19, Me-20; Me-19/H-9a, H-10a; Me-20/H-10a, showed that H-7, H-11, Me-17, Me-19 and Me-20 were both in β, thus, rendering the 7,8-oxirane, and the acetyl group at C-11 to be α orientations (Fig. 3). Additionally, the large coupling constant of $J_{H\text{-}7,H\text{-}6a}$ = 8.8 Hz, $J_{H\text{-}6a,H\text{-}6b}$ = 13.6 Hz, $J_{H\text{-}11,H\text{-}10b}$ = 10.8 Hz, as well as the little coupling of H-7/H-6b and H-11/H-10b, ascertained the α orientations for the epoxy ring at C_7–C_8 and the acetyl group at C-11. Based on the NOE correlations of H-3/H-6b, H-11, Me-19, and Me-18/H-2b, the olefinic geometry of C-3/C-4 was ascertained as *E* form. Hence, the structure of **8** was defined as (1*S*,7*R*,8*S*,11*R*,12*R*,8*Z*)-1:12,7:8-diepoxy-11-acetoxy-5-oxo-3-cembranene (boscartins AO) with the aid of a computer-modeled 3D structure (Fig. 3) generated by MM2 force field calculations for energy minimization using the molecular modeling program Chem 3D Ultra 14.0, as well as the biogenetic consideration.

The two known compounds, boscartins Q (**9**)[3] and boscartins Z (**10**)[3] were identified by comparison of their spectroscopic data (^{1}H and ^{13}C NMR, MS) with the literature values.

A speculative biogenetic pathway for all the isolated compounds except **2** was shown in Fig. 4. Incensole obtained as the main cembrane-type diterpenoid from the gum resin of *B. carterii*,[14,18–20] is proposed as the precursor for the other cembranes, which gradually acetylized, oxidized, and isomerized to their derivatives. Isolated compounds (**1–10**) were examined for the antiproliferative activity against HCT-116 human colon cancer cell, anti-inflammatory activity against nitric oxide (NO) production, and hepatoprotective activity, with cisplatin (5.6 μM), dexamethasone (2.2 μM), and bicyclol being used as the positive controls, respectively. All of them showed weak antiproliferative activity (IC_{50} > 100 μM), and **8** exhibited potent inhibitory effects on NO production (IC_{50} of 14.8 μM), with the others showing weak anti-inflammatory activity (IC_{50} > 30 μM), and all compounds except for **7** and **8** exhibited hepatoprotective activity at 10 μM (Table 3), among which **1** exhibited more potent hepatoprotective activity than the positive control, bicyclol, against the damage induced by

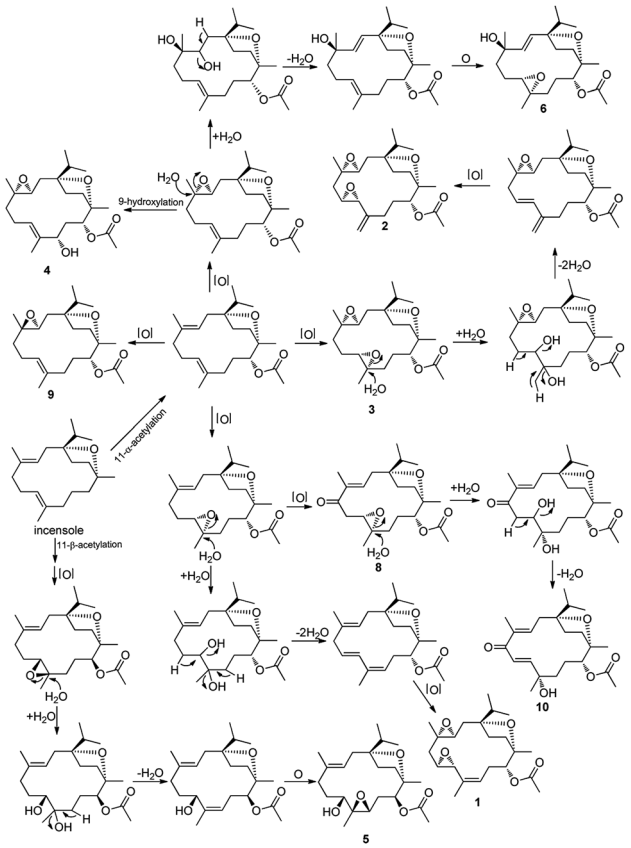

Fig. 4 Speculative biogenetic pathways for the isolated compounds.

Table 3 Protective effects of compounds **1–10** (10 μM) against cytotoxicity induced by paracetamol in HepG2 cells[a]

No.	Cell viability (% of blank)	Inhibition rate (%)
Blank	100	
Control	50.8	
Bicyclol	67.7[b]	27.8
1	75.5[c] < 0.001	45.7
2	68.0[b] < 0.01	21.0
3	57.5	6.1
4	63.6[c] < 0.001	13.6
5	51.9	2.5
6	61.8[c] < 0.001	9.3
7	49.4	−2.9
8	44.0	−4.6
9	62.9[d] < 0.05	12.9
10	64.1[c] < 0.001	14.0

[a] Results were expressed as the means ± SD (n = 3 for blank, control, bicyclol and all isolated compounds); bicyclol was used as the positive control (10 μM). [b] P < 0.01, compared with control group. [c] P < 0.001, compared with control group. [d] P < 0.05 compared with control group.

paracetamol in HepG2 cells (inhibition rate of 45.7%), with **2** exhibiting slightly lower hepatoprotective activity than bicyclol (inhibition rate of 21.0%).

3. Experimental section

3.1. General experimental procedures

Optical rotations were obtained using a SEEWE SGW-2 digital polarimeter in MeOH. HRESIMS were determined on a Bruker Impact II mass spectrometer. IR spectra were collected using a Nicolet 5700 spectrometer. NMR spectra were determined using a BURKER 400 NMR in $CDCl_3$ and DMSO-d_6. Silica gel (200–300 mesh) and ODS C_{18} silica gel (YMC Co., Ltd., Japan) were used for column chromatography (CC) separation. Semi-preparative CC separations were carried out using a Shimadzu LC-6AD instrument, in association with a SPD-10A detector and a reversed-phase C_{18} column (YMC-Pack ODS-AU 20 × 250 mm, 10 μm). All solvents used were of analytical grade.

3.2. Plant material

Olibanum, the gum resin of *Boswellia carterii* Birdw., used in this study were the same as those in our previous study,[21,22] as well as the medicine origin.

3.3. Extraction and isolation

The gum resin of *B. carterii* (6 kg) was extracted with 95% EtOH, which were portioned subsequently with petroleum ether (PE), CH_2Cl_2, EtOAc, and *n*-BuOH as previously described.[19,20] The combined PE fraction (2000 g) was further separated by CC over silica gel rapidly eluted with PE, CH_2Cl_2 and EtOAc. The eluted PE fraction was combined together and further separated by silica gel CC eluted with gradient solvents of PE–EtOAc (100 : 0 → 0 : 1) to yield 4 fractions. Fraction 1 [PE–EtOAc (50 : 1), 14.0 g] was applied to silica gel CC eluted with gradient solvents of PE–EtOAc (100 : 0 → 25 : 1) to yield 11 fractions (F1-1–F1-11). F1-2 [PE–EtOAc (25 : 1), 20 mg] was separated by preparative HPLC system [mobile phase: CH_3CN/H_2O (90%); flow rate: 3 mL min^{-1}; UV detection at 210] resulting in the isolation of **7** (12 mg). F1-3 [PE–EtOAc (25 : 1), 200 mg] was separated by preparative HPLC system [mobile phase: CH_3CN/H_2O (90%); flow rate: 5 mL min^{-1}; UV detection at 210] resulting in the isolation of **9** (78 mg). F1-6 [PE–EtOAc (10 : 1), 80 mg] was separated by preparative HPLC system [mobile phase: CH_3CN/H_2O (70%); flow rate: 5 mL min^{-1}; UV detection at 210] resulting in the isolation of **1** (25 mg) and **2** (21 mg). F1-7 [PE–EtOAc (10 : 1), 65 mg] was separated by preparative HPLC system [mobile phase: CH_3CN/H_2O (70%); flow rate: 5 mL min^{-1}; UV detection at 230] resulting in the isolation of **3** (20 mg) and **8** (5 mg). F1-9 [PE–EtOAc (5 : 1), 80 mg] was separated by preparative HPLC system [mobile phase: CH_3CN/H_2O (65%); flow rate: 5 mL min^{-1}; UV detection at 210] resulting in the isolation of **4** (13 mg), **5** (6 mg) and **6** (40 mg). Fraction 3 [PE–EtOAc (15 : 1), 15.0 g] was applied to silica gel CC eluted with gradient solvents of PE–EtOAc (100 : 0 → 25 : 1) to yield 10 fractions (F3-1–F3-10). F3-6 [PE–EtOAc (3 : 1), 10 mg] was separated by preparative HPLC system [mobile phase: CH_3CN/H_2O (55%); flow rate: 5 mL min^{-1}; UV detection at 230] resulting in the isolation of **10** (4 mg).

3.3.1. Boscartins AH (1). Colorless oil (CH_3OH–$CHCl_3$); $[\alpha]_{25}^{D} = -40.9°$ (*c* 0.67, $CHCl_3$); IR (KBr) ν_{max}: 3476, 2961, 2927, 2875, 1736, 1466, 1372, 1234, 1108, 1024 cm^{-1}; ^1H NMR ($CDCl_3$, 400 MHz) and ^{13}C NMR ($CDCl_3$, 100 MHz), see Table 1; HRESI-MS (positive mode) *m*/*z*: 379.2505 $[M + H]^+$ (calcd for $C_{22}H_{35}O_5$, 379.2440).

3.3.2. Boscartins AI (2). Colorless oil (CH_3OH–$CHCl_3$); $[\alpha]_{25}^{D} = +31.8°$ (*c* 0.67, $CHCl_3$); IR (KBr) ν_{max}: 3395, 2954, 2872, 1733, 1467, 1378, 1370, 1234, 1047, 1022 cm^{-1}; ^1H NMR ($CDCl_3$, 400 MHz) and ^{13}C NMR ($CDCl_3$, 100 MHz), see Table 1; HRESI-MS (positive mode) *m*/*z*: 379.2521 $[M + H]^+$ (calcd for $C_{22}H_{35}O_5$, 379.2440).

3.3.3. Boscartins AJ (3). Colorless oil (CH_3OH–$CHCl_3$); $[\alpha]_{25}^{D} = +7.8°$ (*c* 0.57, $CHCl_3$); IR (KBr) ν_{max}: 3455, 2958, 2925, 1734, 1463, 1376, 1241, 1082, 1039 cm^{-1}; ^1H NMR ($CDCl_3$, 400 MHz) and ^{13}C NMR ($CDCl_3$, 100 MHz), see Table 1; HRESI-MS (positive mode) *m*/*z*: 381.2653 $[M + H]^+$ (calcd for $C_{22}H_{37}O_5$, 381.2596).

3.3.4. Boscartins AK (4). Colorless oil (CH_3OH–$CHCl_3$); $[\alpha]_{25}^{D} = +12.5°$ (*c* 0.37, $CHCl_3$); IR (KBr) ν_{max}: 3454, 3293, 2964, 2921, 1737, 1456, 1365, 1234, 1101, 1048, 1031 cm^{-1}; ^1H NMR ($CDCl_3$, 400 MHz) and ^{13}C NMR ($CDCl_3$, 100 MHz), see Table 1; HRESI-MS (negative mode) *m*/*z*: 379.2357 $[M - H]^-$ (calcd for $C_{22}H_{35}O_5$, 381.2596).

3.3.5. Boscartins AL (5). Colorless oil (CH_3OH–$CHCl_3$); $[\alpha]_{25}^{D} = +40.5°$ (*c* 0.11, $CHCl_3$); IR (KBr) ν_{max}: 3425, 2973, 2932, 1731, 1443, 1375, 1239, 1110, 1049, 1026, 1006 cm^{-1}; ^1H NMR ($CDCl_3$, 600 MHz) and ^{13}C NMR ($CDCl_3$, 125 MHz), see Table 2; HRESI-MS (positive mode) *m*/*z*: 381.2635 $[M + H]^+$ (calcd for $C_{22}H_{37}O_5$, 381.2596).

3.3.6. Boscartins AM (6). Colorless oil (CH_3OH–$CHCl_3$); $[\alpha]_{25}^{D} = +17.0°$ (*c* 1.00, $CHCl_3$); IR (KBr) ν_{max}: 3427, 2964, 2930, 1733, 1461, 1373, 1241, 1028 cm^{-1}; ^1H NMR (DMSO-d_6, 400 MHz) and ^{13}C NMR (DMSO-d_6, 100 MHz), see Table 2; HRESI-MS (positive mode) *m*/*z*: 403.2455 $[M + Na]^+$ (calcd for $C_{22}H_{36}O_5Na$, 403.2460).

3.3.7. Boscartins AN (7). Colorless oil (CH_3OH–$CHCl_3$); $[\alpha]_{25}^{D} = -27.9°$ (*c* 0.33, $CHCl_3$); IR (KBr) ν_{max}: 3442, 2956, 2923, 1731, 1462, 1376, 1241, 1100, 1032 cm^{-1}; ^1H NMR ($CDCl_3$, 400 MHz) and ^{13}C NMR ($CDCl_3$, 100 MHz), see Table 2; HRESI-MS (positive mode) *m*/*z*: 385.2346 $[M + Na]^+$ (calcd for $C_{22}H_{34}O_4Na$, 385.2355).

3.3.8. Boscartins AO (8). Colorless oil (CH_3OH–$CHCl_3$); $[\alpha]_{25}^{D} = -12.0°$ (*c* 0.13, $CHCl_3$); IR (KBr) ν_{max}: 3448, 2971, 1737, 1687, 1619, 1445, 1373, 1237, 1112, 1046, 1026 cm^{-1}; ^1H NMR ($CDCl_3$, 400 MHz) and ^{13}C NMR ($CDCl_3$, 100 MHz), see Table 2; HRESI-MS (positive mode) *m*/*z*: 379.2487 $[M + H]^+$ (calcd for $C_{22}H_{35}O_5$, 379.2440).

3.4. Biological assays

3.4.1. Antiproliferative assessment. Compounds **1–10** were screened for the antiproliferative activity against HCT-116 human colon cancer cell by the MTT method used previously in our study.[21,22]

3.4.2. Anti-inflammatory activity assay against NO production. Compounds **1–10** were assayed for the inhibitory activity against NO production in RAW264.7 mouse peritoneal macrophages by the method used previously in our study.[21,22]

3.4.3. Protective effect on cytotoxicity induced by paracetamol in HepG2 cells. Compounds **1–10** were investigated for the hepatoprotective activity in HepG2 cells by the MTT method used previously.[23,24] HepG2 cells were planted in 96-well plates at a density of 1×10^4 per well and incubated in 100 μL RPMI 1640 for 24 h with the conditions of 37 °C and 5% CO_2. To calculate the IC_{50} values of **1–10**, firstly five varied concentrations of samples (20, 10, 5, 2.5, 1.25 μM) were administered to the HepG2 cells for 1 h with bicyclol used as the positive control. And then the cytotoxicity of the cultured cells was induced by adding paracetamol (concentration of 8 μM). After 48 h of treatment, the cell supernatants were discarded and 100 μL MTT (concentration of 0.5 mg mL^{-1}) was added to the cells to form formazan. Four hours later, 100 μL DMSO was added after discarding the supernatants. The resulted optical density values of each well were measured at 490 nm. The inhibition rate is designated as below:

$$\text{Inhibition rate (\%)} = [(\text{OD(test)} - \text{OD(control)})/(\text{OD(blank)} - \text{OD(control)})] \times 100\%.$$

4. Conclusions

As part of an ongoing research for cembrane-type diterpenoids with diverse structures and significant activities from the gum resin of *Boswellia carterii*, a phytochemical investigation of the petroleum ether extract was conducted, leading the isolation of eight new cembrane-type diterpenoids, boscartins AH-AK (**1–8**), along with two known ones (**9-10**). These eight undescribed cembranoids were characteristic of high oxidation assignable to either three or two epoxy groups connected to the 14-membered acrocycle, as well as a acetyl group at C-11. All isolates were evaluated for antiproliferative activity against HCT-116 human colon cancer cell and anti-inflammatory activity against nitric oxide (NO) production *in vitro*. All of them showed weak antiproliferative activity ($IC_{50} > 100$ μM), and **8** exhibited potent inhibitory effects on NO production (IC_{50} of 14.8 μM), with the others showing weak anti-inflammatory activity ($IC_{50} > 30$ μM), and all compounds except for **7** and **8** exhibited hepatoprotective activity at 10 μM. Results of the inhibitory effects on NO production indicated that a keto functionality in the structure might play an important role for anti-inflammatory activity. As for the hepatoprotective activity, compound **1** exhibited more potent hepatoprotective activity than the positive control, with **2** exhibiting slightly lower hepatoprotective activity than bicyclol, which indicated that three epoxy groups and a double bond in the structure might play an important role for hepatoprotective activity. This study not only provided abundant categories of cembrane-type diterpenoids in gum resin of *Boswellia carterii*, but also dug out the potential active functionality for further structural modification of these cembranoids.

Conflicts of interest

There are no conflicts to declare.

Acknowledgements

We thank associate Professor Fengqin Zhou for the sample authentication. This work was supported by Shandong Provincial Natural Science Foundation, China (ZR2018QH006), Shandong Provincial Key Research and Development Plan (2019GSF108004), and The Priority Research Program of the Shandong Academy of Sciences.

References

1 Committee of the Chinese Pharmacopia, *The Chinese Pharmacopeia*, China Medical Science Press, Beijing, 2015, vol. 1, p. 223.
2 J. J. Wang, B. Zheng, J. W. Hu, M. J. Shi, C. J. Wei, X. Wang, H. Sun and T. F. Ji, *Phytochemistry*, 2019, **163**, 126–131.
3 Y. G. Wang, J. Ren, J. Ma, J. B. Yang, T. F. Ji and A. G. Wang, *Fitoterapia*, 2019, **137**, 104263.
4 H. P. T. Ammon, *Phytomedicine*, 2019, **63**, 153002.
5 J. Q. Yu, H. W. Zhao, D. J. Wang, X. Y. Song, L. Zhao and X. Wang, *J. Sep. Sci.*, 2017, **40**, 2732–2740.
6 S. Bahramzadeh, M. Tabarsa, S. G. You, K. Yelithao, V. Klochkov and R. Ilfat, *J. Funct. Foods*, 2019, **52**, 450–458.
7 B. A. Shah, G. N. Qazi and S. C. Taneja, *Nat. Prod. Rep.*, 2009, **26**, 72–89.
8 B. Prakash, P. K. Mishra, A. Kedia and N. K. Dubey, *LWT–Food Sci. Technol.*, 2014, **56**, 240–247.
9 C. L. Woolley, M. M. Suhail, B. L. Smith, K. E. Boren, L. C. Taylor, M. F. Schreuder, J. K. Chai, H. Casabianca, S. Haq, H.-K. Lin, A. A. Al-Shahri, S. Al-Hatmi and D. G. Young, *J. Chromatogr. A*, 2012, **1261**, 158–163.
10 S. L. Su, Y. Q. Hua, Y. Y. Wang, W. Gu, W. Zhou, J. A. Duan, H. F. Jiang, T. Chen and Y. P. Tang, *J. Ethnopharmacol.*, 2012, **139**(2), 649–656.
11 M. E. F. Hegazy, T. A. Mohamed, A. I. Elshamy, A. R. Hamed, M. A. A. Ibrahim, S. Ohta, A. Umeyama, P. W. Paré and T. Efferth, *RSC Adv.*, 2019, **9**, 27183.
12 C. Angulo-Preckler, G. Genta-Jouve, N. Mahajan, M. D. L. Cruz, N. D. Pedro, F. Reyes, K. Iken, C. Avila and O. P. Thomas, *J. Nat. Prod.*, 2016, **79**, 1132–1136.
13 N. U. Rehman, H. Hussain, S. Al-Shidhani, S. K. Avula, G. Abbas, M. U. Anwar, M. Górecki, G. Pescitelli and A. Al-Harrasi, *RSC Adv.*, 2017, **7**, 42357–42362.
14 A. Al-Harrasi, R. Csuk, A. Khan and J. Hussain, *Phytochemistry*, 2019, **161**, 28–40.
15 W. N. Setzer, *J. Mol. Model.*, 2018, **24**, 74.
16 F. Pollastro, S. Golin, G. Chianese, M. Y. Putra, A. S. Moriello, L. D. Petrocellis, V. García, E. Munoz, O. Taglialatela-Scafati and G. Appendino, *J. Nat. Prod.*, 2016, **79**, 1762–1768.
17 J. Ren, Y. G. Wang, A. G. Wang, L. Q. Wu, H. J. Zhang, W. J. Wang, Y. L. Su and H. L. Qin, *J. Nat. Prod.*, 2015, **78**, 2322–2331.

18 S. Al-Shidhani, N. U. Rehman, F. Mabood, M. Al-Broumi, H. Hussain, J. Hussain, R. Csuk and A. Al-Harrasi, *Phytochem. Anal.*, 2018, **29**, 300–307.
19 S. K. Avula, H. Hussain, R. Csuk, S. Sommerwerk, P. Liebing, M. Górecki, G. Pescitelli, A. Al-Rawahi, N. U. Rehman, I. R. Green and A. Al-Harrasi, *Tetrahedron: Asymmetry*, 2016, **27**, 829–833.
20 S. I. Ali, C. R. Zhang, A. A. Mohamed, F. K. EL-Baz, A. K. Hegazy, M. A. Kord and M. G. Nair, *Nat. Prod. Commun.*, 2013, **8**, 1934578X1300801.
21 J. Q. Yu, Y. L. Geng, H. W. Zhao and X. Wang, *Tetrahedron*, 2018, **74**, 5858–5866.
22 J. Q. Yu, Y. L. Geng, D. J. Wang, H. W. Zhao, L. P. Guo and X. Wang, *Phytochem. Lett.*, 2018, **28**, 59–63.
23 N. L. Zhu, H. F. Wu, Z. Q. Xu, C. Q. Liu, Y. Tian, M. G. Hu, Z. H. Sun, P. F. Li, G. X. Ma and X. D. Xu, *RSC Adv.*, 2017, **7**, 41495–41498.
24 G. J. Balachander, S. Subramanian and K. Ilango, *RSC Adv.*, 2018, **8**, 26656–26663.